Research in Astronomy and Astrophysics, 23:075018 (8pp), 2023 July https://doi.org/10.1088/1674-4527/acc91b

Speckle-interferometric Study of Close Visual Binary System HIP 11253 (HD 14874) using Gaia (DR2 and EDR3)

Hussam Aljboor[1] and Ali Taani[2]
[1] Department of Basic Scientific Sciences, Prince Hussein Bin Abdullah II Academy for Civil Protection, Al Balqa Applied University, Amman, Jordan; hussamaljboor@bau.edu.jo
[2] Physics Department, Faculty of Science, Al Balqa Applied University, 19117 Salt, Jordan; ali.taani@bau.edu.jo
Received 2022 November 4; revised 2022 December 19; accepted 2023 January 11; published 2023 June 20

Abstract

We present a comprehensive set of physical and geometrical parameters for each of the components of the close visual binary system HIP 11253 (HD 14874). We present an analysis for the binary and multiple stellar systems with the aim to obtain a match between the overall observational spectral energy distribution of the system and the spectral synthesis created from model atmospheres using Al-Wardat's method for analyzing binary and multiple stellar systems. The epoch positions are used to determine the orbital parameters and the total mass. The parameters of both components are derived as: $T_{\rm eff}^{\rm a} = 6025$, $T_{\rm eff}^{\rm b} = 4710$, $\log g_{\rm a} = 4.55$, $\log g_{\rm b} = 4.60$, $R_{\rm a} = 1.125\ R_{\odot}$, $R_{\rm b} = 0.88\ R_{\odot}$, $L_{\rm a} = 1.849\ L_{\odot}$, $L_{\rm b} = 0.342\ L_{\odot}$. Our analysis shows that the spectral types of the components are F9 and K3. By combining the orbital solution with the parallax measurements of Gaia DR2 and EDR3, we estimate the individual masses using the H-R diagram as $M_{\rm a} = 1.09\ M_{\odot}$ and $M_{\rm b} = 0.59\ M_{\odot}$ for using Gaia DR2 parallax and $M_{\rm a} = 1.10\ M_{\odot}$ and $M_{\rm b} = 0.61\ M_{\odot}$ for using Gaia EDR3 parallax. Finally, the location of both system's components on the stellar evolutionary tracks is presented.

Key words: (stars:) binaries: visual – stars: kinematics and dynamics – (stars:) binaries (including multiple): close – techniques: interferometric – techniques: spectroscopic

1. Introduction

About half of the stars in the Galaxy are binaries or stellar systems (Duquennoy & Mayor 1991; Cai et al. 2012). The analysis of binary systems is an efficient method for determining their physical and geometrical properties, such as the stellar masses. Close Visual Binary Stars (CVBSs) are binaries with a small separation angle (1″ or less) between their components, and they are hard to detect with a small telescope. Since the long orbital periods of CVBSs have a range of 10–1000 yr, it takes a long time to observe one orbital period (Jiang et al. 2013; Taani et al. 2019). The visual binaries are an important source to obtain the masses and distances of the stars, which contribute to the understanding of their basic physical properties (Taani & Vallejo 2017; Taani et al. 2022a, 2022b). The recent measurements of such systems by the Gaia astrometry mission with increased precision have improved the distances to such systems (Collaboration 2018; Mardini et al. 2019a, 2019b, 2020; Brown et al. 2021). The system HIP 11253, being visually close enough, enables accurate measurements of its colors, color indices, and magnitude difference between its components.

In this paper, we use two methods. The first one is Al-Wardat's method for analyzing binary and multiple stellar systems (BMSSs), which was introduced by Al-Wardat (2002), and has been used to analyze many CVBSs and BMSSs (Al-Wardat & Widyan 2009; Al-Wardat 2012; Masda et al. 2019; Widyan & Aljboor 2021; Al-Tawalbeh et al. 2021; Al-Wardat et al. 2021; Abu-Dhaim et al. 2022). The main idea of Al-Wardat's method is to build entire spectral energy distributions (SEDs) of BMSSs using the model atmospheres like those of (ATLAS9) (Kurucz 1994), by implementing the available observational measurements like magnitude difference and color indices. The second method is Tokovinin's method for the dynamical analysis of binary stars (Tokovinin 1992), which was used to solve the orbit of the system. Details of this program can be found in Tokovinin (2017).

HIP 11253 is located at an R.A. of $02^{\rm h}20^{\rm m}51^{\rm s}$ and decl. of $+30°38'48''$ (SIMBAD catalog). The parallax of the system is obtained from the Gaia Data Release 2 (DR2) (Collaboration 2018) with a value of 18.9878 ± 0.627 mas, which corresponds to a distance of 52.67 pc, and the Gaia Early Data Release 3 (EDR3) (Brown et al. 2021) value is 18.1854 ± 0.213 mas, which corresponds to a distance of 54.99 pc. Table 1 contains the basic information on the system from SIMBAD and other databases.

The aim of this study is to find reliable stellar parameters for systems that may produce the best agreement between measured magnitudes and color indices and synthetic results. In addition, we use the Gaia DR2 parallaxes (Collaboration 2018) and Gaia EDR3 parallaxes (Brown et al. 2021). We emphasize that the

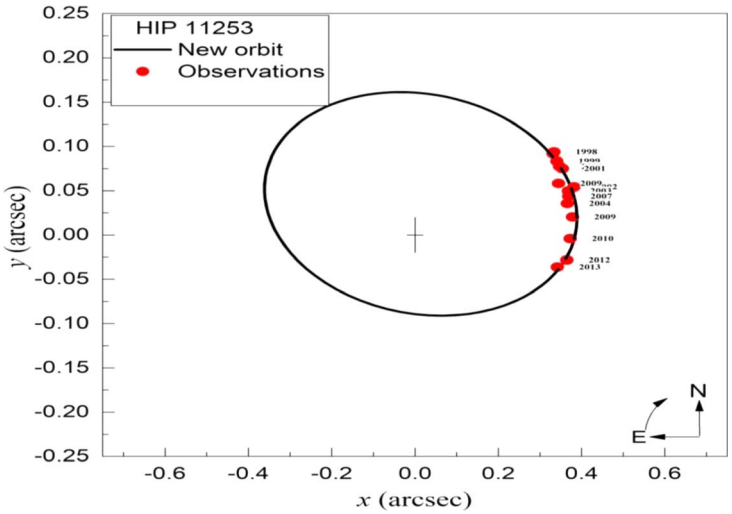

Figure 1. The relative orbit of the binary system HIP 11253 constructed using the relative position. The measurements were taken from the Fourth Catalog of Interferometric Measurements of Binary Stars.

Table 1
Basic Parameters and Observed Astrometric and Photometric Data of HIP 11253

Property	Parameter	Value	Reference
Position	α_{2000}	$02^h20^m51^s$	http://simbad.u-strasbg.fr/simbad/
	δ_{2000}	$+30^\circ\ 38'48''$	http://simbad.u-strasbg.fr/simbad/
Magnitude (mag)	m_v	8.16	ESA (1997)
	A_v	0.2432	Schlafly & Finkbeiner (2011)
	$(B-V)_J$	0.665 ± 0.018	ESA (1997)
	B_T	8.96 ± 0.012	Hog et al. (2000)
	V_T	8.23 ± 0.010	Hog et al. (2000)
Parallax (mas)	π_{GDR2}	18.9878 ± 0.627	Brown et al. (2018)
	π_{GEDR3}	18.1854 ± 0.213	Brown et al. (2021)

binary system HIP 11253 is presented as an example of how to use the approach mentioned above in the case of a visual close binary with low total mass.

2. Orbital Elements

The determination of the orbital elements is crucial in calculating the stellar masses. The orbit of the HIP 11253 system is obtained using the position angles (θ) and angular separations (ρ) obtained from the Fourth Catalog of Interferometric Measurement of Binary Stars (INT4) (see Table 3), following Tokovinin's method (Tokovinin 1992). The orbit is drawn in Figure 1, and the results of the dynamical analysis and orbital solutions of HIP 11253 are listed in Table 4.

Table 4 shows a good agreement between our estimated orbital period (P); inclination (i); semimajor axis (a); eccentricity (e); position angle of nodes (Ω); argument of periastron (ω); and time of primary minimum (T) with previously reported results.

Figure 2 depicts the new orbit in comparison to the old one obtained earlier by Ling (2011). We estimated the total dynamical mass for this binary system using Kepler's third law. The total dynamical mass is given by

$$M_{\rm Dyn} = M_A + M_B = \left(\frac{a}{\pi}\right)^3 \frac{M_\odot}{P^2}, \quad (1)$$

where a is the semimajor axis in arcsec, π is the trigonometric parallax in arcsec, M_A, M_B are the masses of the individual components, $M_{\rm dyn}$ is the dynamical mass sum, P is the relative orbital period and $M_\odot$ is the mass of the Sun equal to 1.9891×10^{30} kg. The error of the dynamical mass sum is given by

$$\frac{\delta_M}{M_{\rm Dyn}} = \sqrt{9\left(\frac{\delta_\pi}{\pi}\right)^2 + 9\left(\frac{\delta_a}{a}\right)^2 + 4\left(\frac{\delta_P}{P}\right)^2}. \quad (2)$$

Using the orbital period and semimajor axis obtained from the orbital solution and parallax measurement, we estimate the dynamical mass as it appears in Table 4.

3. Atmospheric Modeling

3.1. Input Parameters

We derive the physical parameters of each component of the binary star system HIP 11253 by following Al-Wardat's method for analyzing BMSSs (Al-Wardat 2002). This is done by creating individual SED models for each system component

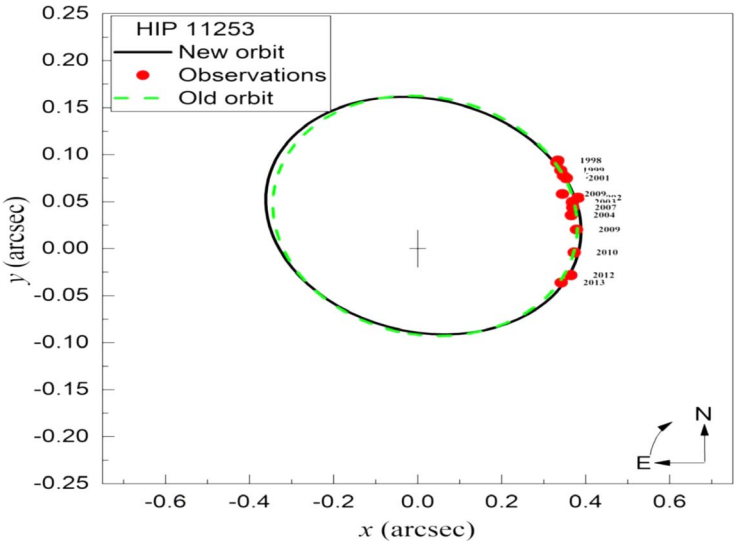

Figure 2. The difference in the orbit between the previous work (Ling 2011) and this work.

Table 2
Magnitude Difference between the Components of the System HIP 11253, along with the Filters used to Obtain the Observations

Δm	Tel*	Filter($\lambda/\Delta\lambda$)	Reference
1.89 ± 0.03	6.0	545 nm/30	Pluzhnik (2005)
2.79 ± 0.22	6.0	545 nm/30	Balega et al. (2006)
2.48 ± 0.19	6.0	600 nm/30	Balega et al. (2006)
2.95 ± 0.00	3.5	550 nm/40	Horch et al. (2008)
2.68 ± 0.05	6.0	540 nm/30	Balega et al. (2007)
2.71 ± 0.00	3.5	550 nm/30	Horch et al. (2009)
2.55 ± 0.00	3.5	562 nm/40	Roberts (2011)

using the visual magnitude $m_v = 8\overset{m}{.}16$ from Table 1, and the average value for visual magnitude band $\Delta m_v = 2\overset{m}{.}16$ from the speckle interferometric results in Table 2, along with parallax of the system ($\pi = 18.9878$, $d = 52.67$ pc) from Gaia DR2, ($\pi = 18.1854$, $d = 54.99$ pc) from Gaia EDR3 and the bolometric corrections (BCs) by Lang (1992). The preliminary specific value of the component input parameters are estimated as expressed in Table 5. To determine the apparent visual magnitude of individual components (m_v^A and m_v^B) we use the following equations:

$$m_v^A = m_v + 2.5 \log (1 + 10^{-0.4 \Delta m_v}), \quad (3)$$

$$m_v^B = m_v^A + \Delta m_v \quad (4)$$

$$M_v = m_v + 5 + 5 \log \pi - A_v. \quad (5)$$

Here A_v is the interstellar extinction coefficient, and π the trigonometric parallax (Brown et al. 2018). The absolute magnitude of individual components (M_v^A and M_v^B) can be calculated according to the equations in Lang (1992) and Gray (2005). With the absolute magnitude, the effective temperature ($T_{\rm eff}$) and the BC can be obtained. The absolute bolometric magnitude ($M_{\rm bol}$) is then calculated using BC.

$$M_{\rm bol} = M_V - {\rm BC} \quad (6)$$

$$M^*_{\rm bol} - M^{\odot}_{\rm bol} = -2.5 \log \left(\frac{L^*}{L_{\odot}} \right). \quad (7)$$

Here $M^{\odot}_{\rm bol}$ is the bolometric magnitude of the Sun $= 4\overset{m}{.}75$, $L_{\odot}$ is luminosity of the Sun $= 3.79 \times 10^{26}$ W, $R_{\odot}$ is the radius of the Sun $= 6.957 \times 10^5$ km, $T_{\odot}$ is the effective temperature of the Sun $= 5777$ K and $M_{\odot}$ is the mass of the Sun 1.988×10^{30} kg.

The radius (R) is obtained through

$$\log \left(\frac{R}{R_{\odot}} \right) = 0.5 \log \left(\frac{L}{L_{\odot}} \right) - 2 \log \left(\frac{T}{T_{\odot}} \right). \quad (8)$$

The gravitational acceleration (logg) is obtained as

$$\log g = \log \left(\frac{M}{M_{\odot}} \right) - 2 \log \left(\frac{R}{R_{\odot}} \right) + 4.43. \quad (9)$$

Note that the $T_{\rm eff}$ and logg values for both components are considered as the preliminary input parameters for both components' atmospheric modeling. As a result, we can compute their synthetic spectra.

3.2. Synthetic Spectra

The input parameters obtained in Section 3.1 are adopted to model the single star's atmosphere by using the corresponding model (ATLAS9) due to Kurucz (1994), while the entire SEDs were built using special subroutines of Al-Wardat's method.

Table 3
New Data on Interferometric Measurements for the HIP 11253 System

Epoch	θ	$\delta\theta$	ρ	$\delta\rho$	mcth	Reference
1991.25	362	.	0.239	.	*Hh*	Hartkopf et al. (1997)
1998.7747	285.6	0.6	0.344	0.004	*S*	Balega et al. (2002)
1998.9246	285.8	.	0.347	.	*S*	Horch et al. (2002)
1999.8130	283.9	0.3	0.351	0.002	*S*	Balega et al. (2004)
2000.8730	282.7	0.5	0.356	0.003	*S*	Balega et al. (2006b)
2001.7528	282.1	0.4	0.362	0.002	*S*	Balega et al. (2006)
2002.7992	278.2	1.1	0.386	0.007	*S*	Balega et al. (2013)
2003.6290	277.8	.	0.372	.	*S*	Horch et al. (2008)
2003.6290	275.7	.	0.368	.	*S*	Horch et al. (2008)
2004.8239	276.9	0.3	0.372	0.002	*S*	Balega et al. (2007)
2007.8256	273.2	.	0.379	.	*S*	Tokovinin et al. (2010)
2009.7371	279.7	21.7	0.350	0.05	*S*	Voitsekhovich & Orlov (2014)
2010.0100	269.5	.	0.373	.	*S*	Horch et al. (2011)
2012.6777	265.7	0.3	0.366	0.009	*S*	Riddle et al. (2015)
2013.7976	264.1	.	0.344	.	*Ag*	Kehrli et al. (2017)

Table 4
Orbital Parameter Solutions and Total Masses Formerly Published for the HIP 11253 System, for Comparison with this Work

Orbital element	Unit	Previous work (Ling 2011)	This work
P	(yr)	82.18	84.48 ± 0.86
ω	(deg)	278.8	276.11 ± 0.27
e	⋯	0.283	0.288 ± 0.0054
Ω	(deg)	87.95	86.95 ± 0.16
i	(deg)	109.7	108.61 ± 0.25
T	(yr)	2026.35	2026.80 ± 0.2184
a	(arcsec)	0.378	0.3921 ± 0.008
M_T[a]	($M_\odot$)	1.1682	1.2342
M_T[b]	($M_\odot$)	1.3297	1.4049
RMS(θ)	(deg)	0.62	0.5907
RMS(ρ)	(arcsec)	0.0124	0.0055

Notes.
[a] Using parallax from Gaia Data Release 2 (DR2).
[b] Using parallax from Gaia Data Release 3 (EDR3).

Table 5
Preliminary Physical and Geometrical Properties of HIP 11253

Parameter	Unit	Gaia Parallax **DR2** (Brown et al. 2018)		Gaia Parallax **EDR3** (Brown et al. 2021)	
		A	B	*A*	*B*
m_v	(mag)	8.30	10.46	8.30	10.64
M_V	(mag)	4.45	6.61	4.36	6.52
BC*	(mag)	−0.09	−0.41	−0.08–0.41	
M_{bol}	(mag)	4.61	7.05	4.44	6.93
T^*_{eff}	(K)	5987	5080	6030	4815
R	($R_\odot$)	2.976	1.342	3.172	1.578
L	($L_\odot$)	1.138	0.120	1.330	0.134
Sp − Type*	⋯	G0	K2	F9	K3

Note. The properties marked by asterisks are obtained using the tables from Lang (1992) and Gray (2005).

Table 6
The Final Results of These Individual Components and the Entire SEDs of the System HIP 11253

HIP 11253 Using		π_{GDR2}	π_{EDR3}
Symbol	Unit		
π	(arcsec)	18.9878	18.1854
d	(pc)	52.67	54.99
R_A	($R_\odot$)	$1.125R_\odot$	$1.175R_\odot$
R_B	($R_\odot$)	$0.88R_\odot$	$0.92R_\odot$
T^A_{eff}	(K)	6025 K	6025 K
T^B_{eff}	(K)	4710 K	4710 K
$\log g_A$	(cm s^{-2})	4.55	4.55
$\log g_B$	(cm s^{-2})	4.60	4.60

Another subroutine of the same method was also used to calculate the individual and entire SEDs. The following equation is used to calculate the synthetic SED as observed from the Earth, which is related to the energy flux of each component (Al-Wardat 2002)

$$F_\lambda.d^2 = H^A_\lambda.R^2_A + H^B_\lambda.R^2_B, \quad (10)$$

which can be expressed as

$$F_\lambda = (R_A/d)^2[H^A_\lambda + H^B_\lambda.(R_B/R_A)^2]. \quad (11)$$

Here, $H^A_\lambda.H^B_\lambda$ are the fluxes at the surface of the star, F_λ is the flux for the entire SED of the binary system, and R_A, R_B are the radii of the primary and secondary components of the system in solar units.

Several works applied an iterative scheme using a different combination of input parameters to get the best fit between the observed flux and the total computed flux (see, i.e., Al-Wardat & Widyan 2009). Additionally, multiple values of Δm, m_v and parallax were applied to achieve convergence. In this way, various models were obtained and compared with the observed

Table 7
Magnitudes and Color Indices of the Entire Synthetic Spectrum and Individual Components of HIP 11253

Sys	Filter	HIP 11253 using					
		Gaia DR2			Gaia EDR3		
		Entire Synth.	A	B	Entire Synth.	A	B
Joh-Cou.	U	8.9891	9.03494	12.4473	8.98816	9.03410	12.4444
	B	8.82499	8.91813	11.5380	8.82400	8.91726	11.5351
	V	8.16179	8.30102	10.4605	8.16070	8.30023	10.4576
	R	7.78665	7.96659	9.82692	7.78549	7.96576	9.82400
	U–B	0.164123	0.116807	0.99328	0.164162	0.116833	0.909332
	B–V	0.663198	0.617116	1.07748	0.663301	0.617037	1.07747
	V–R	0.375146	0.334431	0.633608	0.375205	0.334466	0.633633
Strom.	u	10.1379	10.1790	13.7147	10.1369	10.1781	13.7118
	v	9.18100	9.25202	12.1776	9.17996	9.25111	12.1748
	b	8.53023	8.64619	11.0157	8.52918	8.64538	11.0128
	y	8.12762	8.27197	10.3894	8.12655	8.27124	10.3864
	u–v	0.956917	0.926981	1.53713	0.956951	0.926999	1.53700
	v–b	0.650767	0.605830	1.16186	0.650776	0.605732	1.16202
	b–y	0.402607	0.374220	0.626360	0.402628	0.374146	0.626321
Tycho.	B_T	8.98668	9.06898	11.8287	8.98571	9.06811	11.8258
	V_T 8.23819	8.37034	10.5902	8.23711	8.36952	10.5873	
	$B_T - V_T$	0.748486	0.698636	1.23847	0.748608	0.698564	1.23848

Table 8
Comparison Between the Observational and Synthetic Magnitudes and Color Indices for Both Systems.

HIP 11253			
Filter	Observed (mag)	Synthetic (This Work using Gaia DR2) (mag)	Synthetic (This Work using Gaia EDR3) (mag)
m_v	8.16	8.16179	8.1607
Δm	2.16	2.15948	2.15737
B_T	8.96 ± 0.012	8.98668	8.98571
V_T	8.23 ± 0.010	8.23819	8.23711
$(B-V)_J$	0.665 ± 0.018	0.663198	0.663301

Note. m_v: visual magnitude of the binary system HIP 11253, Δm: the speckle interferometric results in V-band, B_T: photometric magnitude in optical B band between 400 and 500 nm Tycho magnitude, V_T: photometric magnitude in optical V band between 500 and 600 nm Tycho magnitude, $(B-V)_J$: color index or magnitude difference between optical B band between 400 and 500 nm and optical V band between 500 and 600 nm Johnson color index. (Synthetic magnitudes were calculated using subroutines of Al-Wardat's method for analyzing BMSSs.)

Table 9
Estimated Physical Parameters of Individual Components for HIP 11253 System Based on Two Parallax Measurements

Component	Using Gaia DR2		Using Gaia EDR3	
	A	***B***	***A***	***B***
$T_{\rm eff}$(K)	6025	4710	6025	4710
$\log g$	4.55	4.60	4.55	4.60
Radius($R_\odot$)	1.125	0.88	1.175	0.92
$L(L_\odot)$	1.8486	0.3422	1.6334	0.3740
$M_{\rm bol}$	4.08	5.91	4.22	5.82
M_V^*	4.16	6.39	4.30	6.30
Sp. Type*	F9	K3	F9	K3
parallax(mas)	18.9878 ± 0.627		18.1854 ± 0.213	
Mass($M_\odot$)**	$M_a = 1.09\ M_\odot$		$M_b = 0.59\ M_\odot$	
	$M_a + M_b = 1.68\ M_\odot$		$M_a = 1.10\ M_\odot$	
	$M_b = 0.61\ M_\odot$		$M_a + M_b = 1.71\ M_\odot$	

Note. The properties marked by asterisks are obtained using the tables from Lang (1992) and Gray (2005), while those with the double asterisks are obtained using the tables from Girardi et al. (2000). Individual masses were estimated using the results of applying Al-Wardat's method for analyzing BMSSs in the system.

SED. The results are presented in Figures 3 and 4 and in Table 6.

The criteria for Al-Wardat's method to find the best fit are based on the following: the inclination of the spectra, maximum values of the fluxes and profiles of the absorption lines. As a consequence, the best fit we have found (see Figures 3 and 4) used the following set of parameters (see Table 6).

However, Table 7 shows the synthetic spectrum for the entire and individual components of HIP 11253. The comparison between the observational and synthetic values for the color index and magnitude differences is listed in Table 8. A good indication of the reliability of the obtained parameters for the different system components is listed in Table 9. In addition,

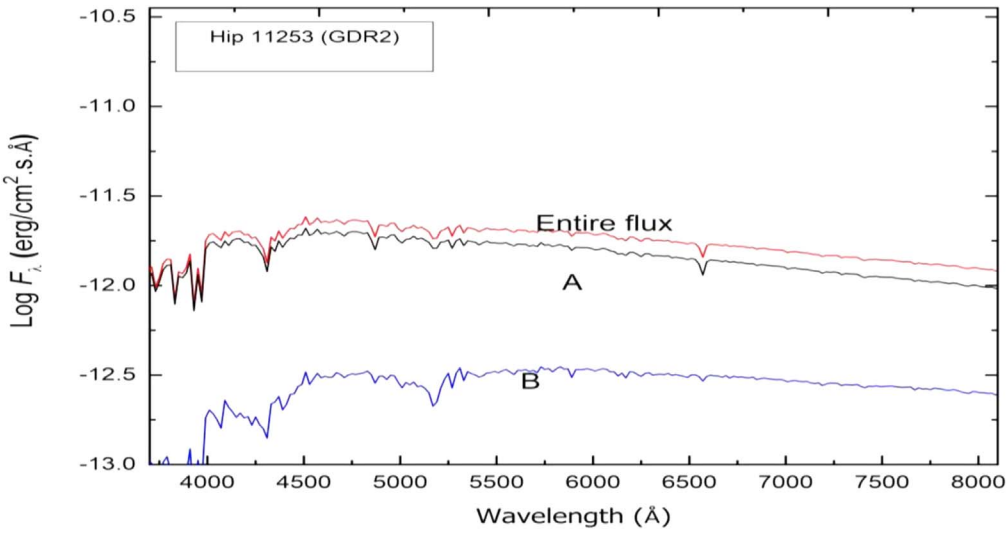

Figure 3. The entire (sum of the fluxes of members A and B) synthetic SED of the system HIP 11253 (built using parameters of the primary component, $T_{\rm eff} = 6025$ K, $\log g = 4.55$ cm s^{-2}, $R = 1.125\,R_\odot$ and the computed flux of the secondary component with $T_{\rm eff} = 4710$ K, $\log g = 4.6055$ cm s^{-2}, $R = 0.88\,R_\odot$ and $d = 54.99$ pc) against the observational one; the figure also shows the synthetic SED for each component.

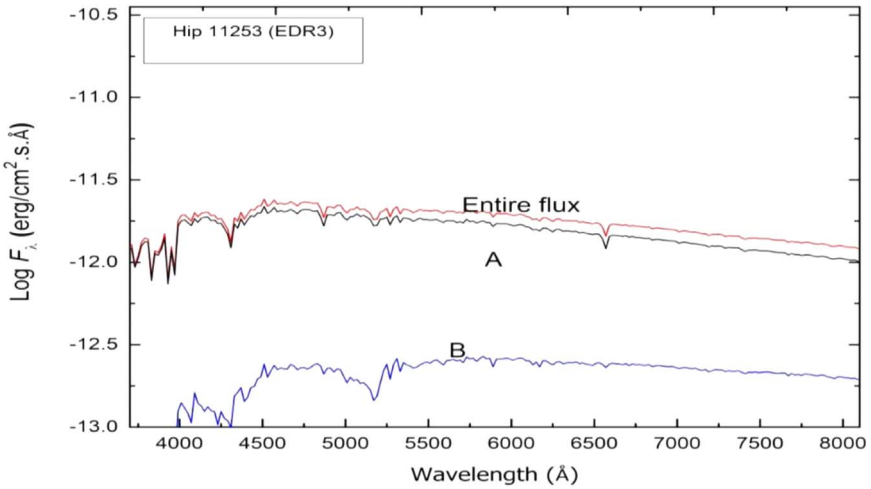

Figure 4. The entire synthetic SED of the system HIP 11253 (built using parameters of the primary component, $T_{\rm eff} = 6025$ K, $\log g = 4.55$ cm s^{-2}, $R = 1.175\,R_\odot$ and the computed flux of the secondary component with $T_{\rm eff} = 4710$ K, $\log g = 4.60\frac{\rm cm}{\rm s^{-2}}$, $R = 092\,R_\odot$ and $d = 52.67$ pc) against the observational one; the figure also shows the synthetic SED for each component.

based on the ultimate effective temperatures of the system, we estimate the bolometric magnitudes and stellar luminosities by using the following equations

$$\log\left(\frac{R}{R_\odot}\right) = 0.5\log\left(\frac{L}{L_\odot}\right) - 2\log\left(\frac{T}{T_\odot}\right). \quad (12)$$

$$\log g = \log\left(\frac{M}{M_\odot}\right) - 2\log\left(\frac{R}{R_\odot}\right) + 4.43. \quad (13)$$

The best fit values are sufficiently representative of the system component parameters. Using Lang (1992) and Gray (2005) empirical relations of spectral types and effective temperature, the spectral types of HIP 11253 components can be obtained as F9 and K3 for components a and b respectively.

4. Synthetic Photometry

Following the treatment by Al-Wardat (2002), the synthetic magnitudes are calculated from the synthetic SED using the

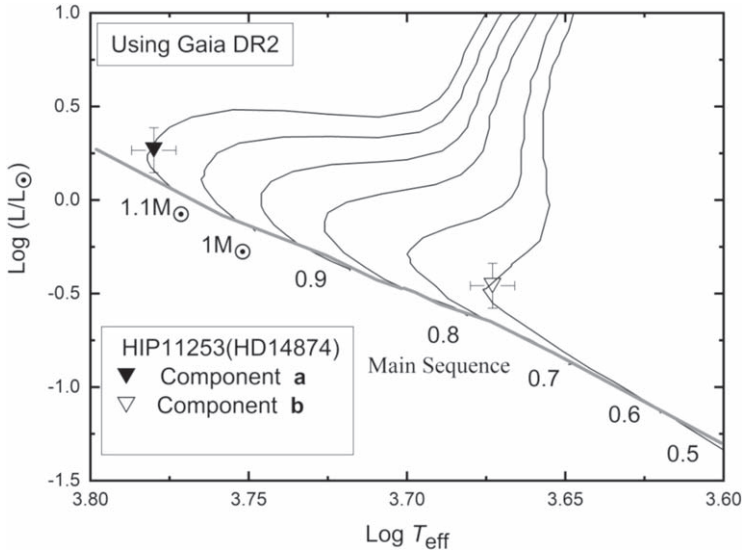

Figure 5. The evolutionary tracks of both components of HIP 11253 on the H-R diagram of masses using Gaia DR2 parallax. The evolutionary tracks were taken from Girardi et al. (2000).

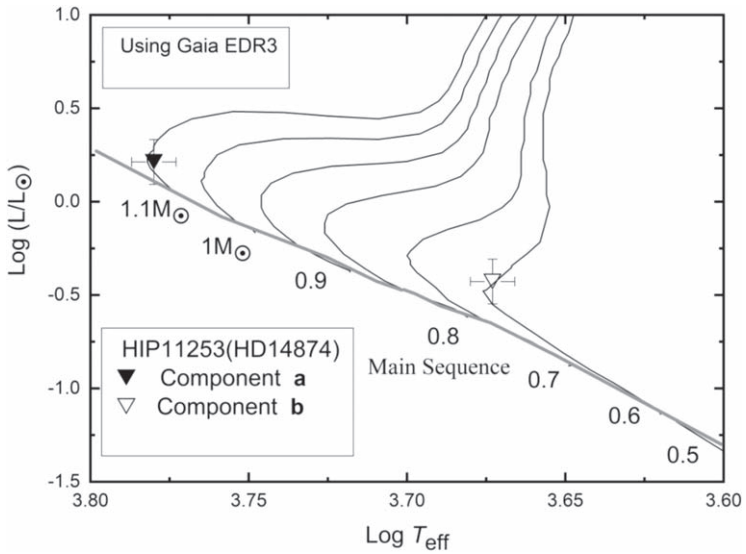

Figure 6. The evolutionary tracks of both components of HIP 11253 on the H-R diagram using Gaia EDR3 parallax. The evolutionary tracks were taken from Girardi et al. (2000).

following relationship

$$m_p[F_{\lambda.s}(\lambda)] = -2.5\log\frac{\int P_p(\lambda)F_{\lambda.s}\lambda d\lambda}{\int P_p(\lambda)F_{\lambda.r}\lambda d\lambda} + ZP_p, \qquad (14)$$

where m_p is the synthetic magnitude of the passband p, $P_p(\lambda)$ is the dimensionless sensitivity function of the passband p, $F_{\lambda.s}(\lambda)$ is the synthetic SED of the object, $F_{\lambda.r}(\lambda)$ is the SED of reference star Vega and ZP_p the zero-point taken from Maíz Apellániz (2007). By using the iteration method with different sets of observed stellar parameters like magnitude differences of the components, color indices of the entire system and individual components in (*U-B-V-R*) Johnson-Cousins, (*uvby*) Strömgren and (*B-V*) Tycho, one can get the best fit between the observational and synthetic magnitudes. This would help us to judge the accuracy of the estimated parameters using a special subroutine of Al-Wardat's method with the Interactive Data Language (IDL) platform and verify the estimated parameter reliability. As we can see, Figures 3 and 4 show best-fittings between the individual components and entire synthetic and observational SED. While on the other hand, Figures 5 and 6 display the evolutionary tracks of a theoretical Hertzsprung-

Russell (H-R) diagram of both the components of HIP 11253, which are evolving off the main sequence. This helps to estimate the masses and spectral types as in Table 9. Al-Wardat's method for analyzing BMSSs gives a mass sum of 1.68 $M_{\odot}$ for Gaia DR2 parallax and 1.71 $M_{\odot}$ for Gaia EDR3 parallax. It is worth noting that masses estimated using this method along with the modified orbital elements are independent of the parallax values. From the comparison of dynamical masses using this approach, we realize that parallax measurement from EDR3 provides a good indication of the mass sum, due to the advance and higher resolution.

5. Conclusions

In this work, we have investigated the basic stellar parameters of the close visual binary system HIP 11253 (HD 14874). Our investigation was based on the following considerations:

(a) Creating individual SED models for each system component as described in Section 3.1 using Al-Wardat's method for analyzing BMSSs (Al-Wardat 2002), combined with the parallax measurements by Gaia (DR2 and EDR3).

(b) The orbital elements were calculated following the dynamical method used by Tokovinin (1992).

(c) We used Al-Wardat's method to calculate the synthetic magnitude, where the results are displayed in Figures 3 and 4.

(d) The spectral types of both components are identified as F9 and K3, for components A and B respectively.

Acknowledgments

The authors used the codes of Al-Wardat's method for analyzing binary and multiple stellar systems.

The authors also thank Mounib Eid for providing his comments and suggestions. The authors would also like to thank the anonymous referee for the careful reading of the manuscript and for all suggestions and comments which allowed us to improve both the quality and the clarity of the paper. This work used the SAO/NASA database, Gaia Data Gaia (DR2 and EDR3), the SIMBAD database, the Fourth Catalog of Interferometric Measurements of Binary Stars and IPAC data systems.

ORCID iDs

Hussam Aljboor https://orcid.org/0000-0001-8463-8068
Ali Taani https://orcid.org/0000-0002-1558-1472

References

Abu-Dhaim, A., Taani, A., Tanineah, D., et al. 2022, AcA, 72, 171
Al-Tawalbeh, Y., Hussein, A., Taani, A., et al. 2021, AstBu, 76, 71
Al-Wardat, M. 2002, Bull. Special Astrophys. Obs, 54, 29
Al-Wardat, M. 2012, PASA, 29, 523
Al-Wardat, M. A., Abu-Alrob, E., Hussein, A., Mardini, M., & Taani, A. 2021, RAA, 21, 161
Al-Wardat, M. A., & Widyan, H. 2009, AstBu, 64, 365
Balega, I. I., Balega, Yu. Yu., Maksimov, A. F., et al. 2006a, Bull. Spec. Astrophys. Obs., 59, 20
Balega, I. I., Balega, Yu. Yu., Hofmann, K.-H., et al. 2002, A&A, 385, 87
Balega, I. I., Balega, Yu. Yu., Hofmann, K.-H., et al. 2006b, A&A, 448, 703
Balega, I. I., Balega, Yu. Yu., Maksimov, A. F., et al. 2007, AstBu, 62, 339
Balega, I. I., Balega, Yu. Yu., Gasanova, L. T., et al. 2013, AstBu, 68, 53
Balega, I., Balega, Yu. Yu., Maksimov, A. F., et al. 2004, A&A, 422, 627
Brown, A. G. A., Vallenari, A., Prusti, T., et al. 2018, A&A, 616, 22
Brown, A. G. A., Vallenari, A., Prusti, T., et al. 2021, A&A, 649, A1
Cai, Y., Taani, A. A., Zhao, Y., et al. 2012, ChJAA, 36, 137
Collaboration 2018, yCat, I-345
Duquennoy, A., & Mayor, M. 1991, A&A, 248, 485
ESA 1997, ESA SP, 1200, F.
Gray, D. F. 2005, The Observation and Analysis of Stellar Photospheres (3rd ed; Cambridge: Cambridge Univ. Press)
Hartkopf, W. I., McAlister, H. A., Mason, B. D., et al. 1997, AJ, 114, 1639
Hog, E., Fabricius, C., Fabricius, V., et al. 2000, A&A, 357, 367
Horch, E. P., Robinson, S. E., Ninkov, Z., et al. 2002, AJ, 124, 2245
Horch, E. P., van Altena, W. F., Cyr Jr, W. M., et al. 2008, AJ, 136, 312
Horch, E. P., Falta, F., Anderson, L. M., et al. 2009, AJ, 139, 205
Horch, E. P., Gomez, S. C., Sherry, W. H., et al. 2011, AJ, 141, 45
Jiang, L., Zhang, C.-M., Tanni, A., et al. 2013, Characteristic Age and True Age of Pulsars, 23 (Singapore: World Scientific), 95
Kehrli, M., David, H., Drake, E., et al. 2017, JDSO, 13, 122
Kurucz, R. 1994, A&A, 281, 817
Lang, K. R. 1992, Astrophysical Data (New York: Springer)
Ling, J. F. 2011, AJ, 143, 20
Maíz Apellániz, J. 2007, The Future of Photometric, Spectrophotometric and Polarimetric Standardization, 364 (Astronomical Society of the Pacific Conference Series: ASP), 227
Mardini, M., Placco, V. M., Taani, A., et al. 2019a, ApJ, 882, 27
Mardini, M., Li, H., Placco, V. M., et al. 2019b, ApJ, 875, 89
Mardini, M., Placco, V. M., Meiron, Y., et al. 2020, ApJ, 903, 88
Masda, S. G., Docobo, J. A., Hussein, A. M., et al. 2019, AstBu, 74, 464
Pluzhnik, E. A. 2005, A&A, 431, 587
Riddle, R. L., Tokovinin, A., Mason, B. D., et al. 2015, ApJ, 799, 4
Roberts, L. C. 2011, MNRAS, 413, 1200
Schlafly, E. F., & Finkbeiner, D. P. 2011, ApJ, 737, 103
Taani, A., Abushattal, A., & Mardini, M. K. 2019, AN, 340, 847
Taani, A., & Vallejo, J. C. 2017, PASA, 34, E024
Taani, A., Vallejo, J. C., & Abu-Saleem, M. 2022a, JHEAp, 35, 83
Taani, A., Karino, S., Song, L., et al. 2022b, PASA, 39, e040
Tokovinin, A. 1992, IAU Colloq. 135: Complementary Approaches to Double and Multiple Star Research, 32, 573
Tokovinin, A. 2017, AJ, 154, 110
Tokovinin, A., Mason, B. D., & Hartkopf, W. I. 2010, AJ, 139, 743
Voitsekhovich, V. V., & Orlov, V. G. 2014, RMxAA, 50, 37
Widyan, H., & Aljboor, H. 2021, RAA, 21, 110